Advances in Science and Technology Research Journal

Advances in Science and Technology Research Journal, 2026, 20(7), 95–115
https://doi.org/10.12913/22998624/218835
ISSN 2299-8624, License CC-BY 4.0

Received: 2026.02.18
Accepted: 2026.05.15
Published: 2026.06.01

Accuracy analysis of aircraft positioning based on dual receiver GPS/EGNOS and GPS/SDCM solution in aerial navigation

Kamil Krasuski[1*], Janusz Jerzy Ćwiklak[1], Adam Ciećko[2], Andrzej Komorek[3], Jacek Janiszewski[3]

[1] Faculty of Navigation and Logistic, Polish Air Force University, ul. Dywizjonu 303 nr 35, 08-521 Dęblin, Poland
[2] University of Warmia and Mazury, Faculty of Geoengineering, ul. Oczapowskiego 2, 10-720 Olsztyn, Poland
[3] Faculty of Aviation, Polish Air Force University, ul. Dywizjonu 303 nr 35, 08-521 Dęblin, Poland
* Corresponding author's e-mail: k.krasuski@law.mil.pl

ABSTRACT

The article presents a methodology for determining the positioning accuracy parameter of GPS with EGNOS and SDCM corrections in air navigation. Namely, the aircraft positioning accuracy parameter was determined as part of a joint GPS/EGNOS+GPS/SDCM solution for two GNSS satellite receivers. The calculation scheme itself was divided into two stages, i.e., first, the accuracy was estimated based on raw GPS/EGNOS+GPS/SDCM data for both GNSS receivers, and then a Kalman filter was applied to improve the determined position of the aircraft, and the accuracy was determined again. The article used the research material collected during an airplane flight around the EPOD airport. The algorithms for the research methodology were written in script in language of Scilab v.6.1.1. During the research, accuracy term was better than 2.94 m. After Kalman filtering, position errors were reduced to 14% for horizontal components and 20% for ellipsoidal height. This allowed for a reduction in position errors below 2.35 m. The paper also calculated other statistical errors, such as: MAE, RMS or standard deviation. In this paper, the characteristics of SBAS corrections were taken into account in terms of determining the accuracy parameter. In particular, the results of SBAS corrections, such as: long-term and fast corrections, ionosphere and troposphere delay. During the research, in addition to accuracy, the availability, continuity, and integrity of GPS/EGNOS+GPS/SDCM positioning in aviation were also calculated. The presented research method can be used in aviation to increase the accuracy term using the SBAS support systems.

Keywords: SBAS, EGNOS, SDCM, aircraft position, accuracy, SBAS corrections.

INTRODUCTION

The last few years have seen dynamic growth in the use of the GNSS satellite systems in aviation navigation in Poland. Furthermore, active development can be observed among the SBAS systems [1]. In Poland, as the history of research on the use of SBAS in air navigation shows, the European EGNOS augmentation system was used as the first SBAS [2]. It should be noted that at that time, only the EGNOS system served as an SBAS augmentation system in this part of Europe. Currently, the number of SBAS systems has also increased [3], covering the territory of Poland with their corrections. This refers primarily to the Russian SDCM augmentation system [4]. The territory of Poland is covered by corrections from both SBAS systems, which can be effectively used in kinematic positioning. The EGNOS and SDCM corrections can be used primarily to improve the absolute positioning of GPS, which directly translates into the determination of the accuracy parameter. Accuracy in this sense should be understood as the difference between the coordinates determined from the GPS/EGNOS (or GPS/SDCM) solution and the reference position of the aircraft flight [5]. In this regard, it should be noted that accuracy is calculated in aviation, alongside continuity, availability, and integrity [6]. The entire study was

devoted to the analysis and examination of this parameter for the EGNOS and SDCM augmentation systems.

In addition to the aforementioned SBAS systems, the British UK SBAS and Algerian AL-SBAS systems also cover the territory of Poland with their corrections [3]. This gives a total of four SBAS systems that can be implemented in air navigation today. On the one hand, the multitude of the SBAS systems allows the user to integrate data, and on the other hand, to control their use with the GPS navigation system. Under the kinematic conditions of GNSS measurement, the ability to use several SBAS systems is extremely valuable for the user. This mainly applies to the use of SBAS systems en route and on approach to landing in accordance with ICAO requirements [6]. It is reasonable for on-board GNSS receivers to be able to record the SBAS corrections from several geostationary satellites, rather than relying on a single SBAS system. Real-time flight tests allow determining how individual corrections from a given SBAS system affect the kinematic position of the flight, which changes at a set time interval.

RELATED WORKS

The analysis of references for the article should be divided into two main parts, i.e., the research conducted in Poland and worldwide, respectively. The first part discusses the characteristics of research on the use of the EGNOS and SDCM support systems in Polish aviation. The characteristics of the research mainly concern the following issues:

- the influence of tropospheric delay on determining the position with the GPS/EGNOS or GPS/SDCM solutions [7],
- research the availability, continuity, accuracy and integrity of the GPS/EGNOS and GPS/SDCM positioning in transport [8],
- determining the accuracy term of single-receiver GPS/EGNOS and GPS/SDCM positioning [9-11],
- determining the precision of user coordinate determination using GPS/EGNOS+GPS/SDCM solutions [12],
- the use of both SBAS support systems to estimate the position of UAVs during flight [13, 14].

In addition, it is also worth mentioning the work [15], which determined the accuracy of static positioning using the GPS/EGNOS and GPS/SDCM solutions. The study was conducted as a typical geodetic measurement.

There are few publications worldwide on the simultaneous use of the EGNOS and SDCM augmentation systems. Both augmentation systems have been used mainly in GNSS satellite navigation or surveying applications. It is worth mentioning publications [4, 16-18], which described the history of the EGNOS and SDCM systems as the SBAS systems in satellite navigation. Publication [19] presented the influence of the EGNOS and SDCM corrections on the determination of GPS and GLONASS positioning accuracy. In this case, the accuracy of determining the coordinates of the GNSS reference stations was within ±1-2 m. Another paper [20] showed the possibilities of using SDCM in aviation operations in Romania in relation to the EGNOS augmentation system. A very interesting numerical solution was presented in [21]. Specifically, selected SBAS correction models for the SDCM, EGNOS, and other augmentation systems were presented and then compared.

With regard to the literature review, it can be concluded that:

- in Poland, both augmentation systems are mainly applied in air transport,
- in Poland, aviation research has mainly focused on determining the accuracy parameter of single-receiver GPS/SBAS positioning,
- in Poland, the EGNOS and SDCM augmentation systems were used to estimate the position of aircraft and UAV,
- worldwide, the number of scientific studies using both the EGNOS and SDCM augmentation systems was small,
- worldwide, both SBAS systems were mainly applied in GNSS satellite navigation,
- globally, the use of both SBAS systems in the field of satellite navigation and geodesy mainly concerned the determination of GNSS reference station coordinates and the determination of their accuracy.

As the literature shows, the missing research topics in the analysis of the state of knowledge include:

- developing a methodology for estimating the accuracy of a dual-receiver GPS/EGNOS+GPS/SDCM solution,
- implementation of algorithms in the analysis of positioning accuracy from a dual-receiver GPS/EGNOS+GPS/SDCM solution,

- integration of position errors from a single GPS/SBAS solution to determine the resultant accuracy for a dual GNSS receiver system,
- determination of SBAS correction characteristics in terms of accuracy parameter determination.

The most important authors' contribution to the development of research in this field concerns:

- designating the accuracy term using the SBAS data for dual receivers positioning,
- applying a Kalman filter to increase the accuracy parameter in kinematic positioning,
- using an arithmetic mean model to determine the accuracy for on-board GNSS receivers,
- developing an algorithm for determining the resultant accuracy for two GNSS receivers,
- conducting a detailed analysis of SBAS corrections during flight test,
- using an weighted mean model to determine the accuracy for on-board GNSS receivers.

METHODOLOGY OF RESEARCH

The main objective of the research was to designate the accuracy of airplane using the GPS and SBAS data. The process of determining accuracy in form of a block diagram is shown in detail in Figure 1. This diagram was used for two satellite receivers installed on the airplane. Each individual GNSS receiver collects the GPS data and SBAS corrections. Then, based on the SPP solution, the position of the GNSS receiver (in this sense, the user's position) is determined [22]. In addition, the flight reference position is determined at this calculation stage [23].

A model of GPS/EGNOS and GPS/SDCM position solution is created for each GNSS receiver, and then the resultant position of the aircraft [24] is determined for two GNSS receivers. Comparing the estimated coordinates from the GPS/SBAS solution and flight reference position allows the accuracy parameter to be calculated in the form of position errors [25]. The discussed calculation process for determining the accuracy parameter [26] is repeated for two or more on-board GNSS receivers. Therefore, it is also worth describing it in mathematical terms. For each GNSS receiver, the accuracy parameter of kinematic coordinates of an aircraft position can be written as follows:

$$\begin{cases} \Delta B_{Rx1} = \dfrac{\sum_1^n \Delta B_{Rx1}^{GPS/i}}{n} \\ \Delta L_{Rx1} = \dfrac{\sum_1^n \Delta L_{Rx1}^{GPS/i}}{n} \\ \Delta h_{Rx1} = \dfrac{\sum_1^n \Delta h_{Rx1}^{GPS/i}}{n} \end{cases} \quad (1)$$

where: ΔB_{Rx1} – position errors of geodetic width component for a single GNSS receiver, calculated as the arithmetic mean for the GPS/EGNOS and also GPS/SDCM solution, ΔL_{Rx1} – position errors of geodetic length component for a single GNSS receiver, calculated as the arithmetic mean for the GPS/EGNOS and also GPS/SDCM solution, Δh_{Rx1} – position errors of ellipsoidal height component for a single GNSS receiver, calculated as the arithmetic mean for the GPS/EGNOS and also GPS/SDCM solution, n – number of position solutions for a single GNSS receiver, in this case n = 2, i – designation of a single SBAS system, in this case i = EGNOS or i = SDCM, $Rx1$ – designation of a single GNSS receiver, $\Delta B_{Rx1}^{GPS/i}$ – position errors for the geodetic width component for a single GPS with SBAS corrections solution for each GNSS receiver, $\Delta L_{Rx1}^{GPS/i}$ – position errors for the geodetic length component for a single GPS with SBAS corrections solution for each GNSS receiver, $\Delta h_{Rx1}^{GPS/i}$ – position errors for the ellipsoidal height component for a single GPS with SBAS corrections solution for each GNSS receiver.

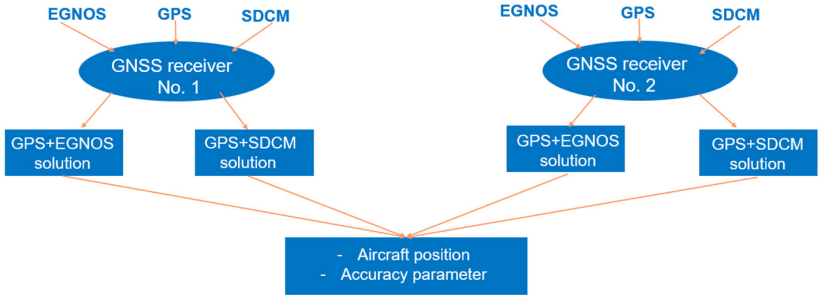

Figure 1. The flowchart of research methodology

Taking into account the number of solutions to Equation 1, we obtain:

$$\begin{cases} \Delta B_{Rx1} = \frac{\Delta B_{Rx1}^{GPS/EGNOS} + \Delta B_{Rx1}^{GPS/SDCM}}{2} \\ \Delta L_{Rx1} = \frac{\Delta L_{Rx1}^{GPS/EGNOS} + \Delta L_{Rx1}^{GPS/SDCM}}{2} \\ \Delta h_{Rx1} = \frac{\Delta h_{Rx1}^{GPS/EGNOS} + \Delta h_{Rx1}^{GPS/SDCM}}{2} \end{cases} \quad (2)$$

where: $\Delta B_{Rx1}^{GPS/EGNOS}$ – position errors for the geodetic width component for a GPS/EGNOS solution for each GNSS receiver, $\Delta L_{Rx1}^{GPS/EGNOS}$ – position errors for the geodetic length component for a GPS/EGNOS solution for each GNSS receiver, $\Delta h_{Rx1}^{GPS/EGNOS}$ – position errors for the ellipsoidal height component for a GPS/EGNOS solution for each GNSS receiver, $\Delta B_{Rx1}^{GPS/SDCM}$ – position errors for the geodetic width component for a GPS/SDCM solution for each GNSS receiver, $\Delta L_{Rx1}^{GPS/SDCM}$ – position errors for the geodetic length component for a GPS/SDCM solution for each GNSS receiver, $\Delta h_{Rx1}^{GPS/SDCM}$ – position errors for the ellipsoidal height component for a GPS/SDCM solution for each GNSS receiver.

On this basis, Equation 2 describes the position errors for each GNSS receiver, assuming the determinability of the GPS/EGNOS and GPS/SDCM solutions. This procedure is used for each on-board GNSS receiver. Therefore, for both GNSS receivers, the accuracy parameter will be determined as follows:

where: ΔB – position errors for the geodetic width component for a system of two GNSS receivers, ΔL – position errors for the geodetic length component for a system of two GNSS receivers, Δh – position errors for the ellipsoidal height component for a system of two GNSS receivers, r – number of GNSS receivers, in this case $r = 2$, $Rx2$ – designation of the second GNSS receiver, $\Delta B_{Rx2}^{GPS/EGNOS}$ - position errors for the geodetic width component for a single GPS/EGNOS solution for the second GNSS receiver, $\Delta L_{Rx2}^{GPS/EGNOS}$ – position errors for the geodetic length component for a single GPS/EGNOS solution for the second GNSS receiver, $\Delta h_{Rx2}^{GPS/EGNOS}$ – position errors for the ellipsoidal height component for a single GPS/EGNOS solution for the second GNSS receiver, $\Delta B_{Rx2}^{GPS/SDCM}$ – position errors for the geodetic width component for a single GPS/SDCM solution for the second GNSS receiver, $\Delta L_{Rx2}^{GPS/SDCM}$ – position errors for the geodetic length component for a single GPS/SDCM solution for the second GNSS receiver, $\Delta h_{Rx2}^{GPS/SDCM}$ – position errors for the ellipsoidal height component for a single GPS/SDCM solution for the second GNSS receiver.

Taking into account the number of solutions for two GNSS receivers in Equations 3, we obtain:

$$\begin{cases} \Delta B = \frac{\frac{\Delta B_{Rx1}^{GPS/EGNOS} + \Delta B_{Rx1}^{GPS/SDCM}}{2} + \frac{\Delta B_{Rx2}^{GPS/EGNOS} + \Delta B_{Rx2}^{GPS/SDCM}}{2}}{r} \\ \Delta L = \frac{\frac{\Delta L_{Rx1}^{GPS/EGNOS} + \Delta L_{Rx1}^{GPS/SDCM}}{2} + \frac{\Delta L_{Rx2}^{GPS/EGNOS} + \Delta L_{Rx2}^{GPS/SDCM}}{2}}{r} \\ \Delta h = \frac{\frac{\Delta h_{Rx1}^{GPS/EGNOS} + \Delta h_{Rx1}^{GPS/SDCM}}{2} + \frac{\Delta h_{Rx2}^{GPS/EGNOS} + \Delta h_{Rx2}^{GPS/SDCM}}{2}}{r} \end{cases} \quad (3)$$

$$\begin{cases} \Delta B = \frac{\Delta B_{Rx1}^{GPS/EGNOS} + \Delta B_{Rx1}^{GPS/SDCM} + \Delta B_{Rx2}^{GPS/EGNOS} + \Delta B_{Rx2}^{GPS/SDCM}}{4} \\ \Delta L = \frac{\Delta L_{Rx1}^{GPS/EGNOS} + \Delta L_{Rx1}^{GPS/SDCM} + \Delta L_{Rx2}^{GPS/EGNOS} + \Delta L_{Rx2}^{GPS/SDCM}}{4} \\ \Delta h = \frac{\Delta h_{Rx1}^{GPS/EGNOS} + \Delta h_{Rx1}^{GPS/SDCM} + \Delta h_{Rx2}^{GPS/EGNOS} + \Delta h_{Rx2}^{GPS/SDCM}}{4} \end{cases} \quad (4)$$

Equation 4 describes the determination of position errors for GPS/SBAS dual-receiver positioning in air navigation. The accuracy specified in Equation 4 represents the integration of position errors calculated from the GPS/EGNOS+GPS/SDCM combination for two GNSS receivers. Therefore, from each GPS/EGNOS and GPS/SDCM solution, there are two position error determinations separately for two GNSS receivers. Hence, the total number of position determinations is four, according to the developed mathematical model. The resultant position of the aircraft is determined with a number of degrees of freedom equal to:

$$f = n - 1 = 4 - 1 = 3 \tag{5}$$

where: f – number of degrees of freedom, n – total number of position assignments.

If, for example, only one GNSS receiver was relied on, then the number of degrees of freedom would be f = n – 1 = 2 – 1 = 1. Therefore, in the developed research methodology, both the number of GPS/SBAS solutions and the number of receivers used in the experiment are important.

The calculated position error results based on Equation 4 may be subject to measurement noise, as the position coordinates from the GPS/EGNOS, GPS/SDCM solution are estimated using the least squares method [27] based on ICAO documents. Therefore, it is advisable to use filtering algorithms to increase the accuracy of GPS/SBAS kinematic solution [28, 29]. For this purpose, a linear Kalman filter was used to increase the position errors of coordinates of the airplane [14, 15] as presented below:

$$\begin{cases} \overline{x}(k) = G \cdot x(k-1) \\ \overline{P}(k) = G \cdot P(k-1) \cdot G^T + Q(k) \end{cases} \tag{6}$$

$$\begin{cases} K(k) = \overline{P}(k) \cdot H^T \cdot \left(H \cdot \overline{P}(k) \cdot H^T + PR\right)^{-1} \\ x(k) = \overline{x}(k) + K(k) \cdot (z - H \cdot \overline{x}(k)) \\ P(k) = (I - K(k) \cdot H) \cdot \overline{P}(k) \end{cases} \tag{7}$$

where: G – coefficient matrix, $G = \begin{bmatrix} 1 & 0 & 0 \\ 0 & 1 & 0 \\ 0 & 0 & 1 \end{bmatrix}$, $x(k-1)$ – estimated values of parameters determined a priori from the previous step, $P(k-1)$ – estimated values of the a priori covariance matrix from the previous step, $P(k-1) = \begin{bmatrix} 10^2 & 0 & 0 \\ 0 & 10^2 & 0 \\ 0 & 0 & 10^2 \end{bmatrix} m^2$, $\overline{x}(k)$ – value forecast, $\overline{P}(k)$ – predicted values of the covariance matrix, $Q(k)$ – covariance matrix of the noise process, $Q(k) = \begin{bmatrix} {w_k}^2 & 0 & 0 \\ 0 & {w_k}^2 & 0 \\ 0 & 0 & {w_k}^2 \end{bmatrix} m^2 = \begin{bmatrix} 10^{-2} & 0 & 0 \\ 0 & 10^{-2} & 0 \\ 0 & 0 & 10^{-2} \end{bmatrix} m^2$ w_k – process noise errors, (k – 1) – previous measurement epoch, k – current measurement epoch, $K(k)$ – Kalman gain matrix, H – partial derivative matrix, $H = \begin{bmatrix} 1 & 0 & 0 \\ 0 & 1 & 0 \\ 0 & 0 & 1 \end{bmatrix}$, PR – covariance matrix of measurements, $PR = \begin{bmatrix} {v_k}^2 & 0 & 0 \\ 0 & {v_k}^2 & 0 \\ 0 & 0 & {v_k}^2 \end{bmatrix} m^2 = \begin{bmatrix} 3 & 0 & 0 \\ 0 & 3 & 0 \\ 0 & 0 & 3 \end{bmatrix} m^2$ v_k – observational model errors, I – unit matrix, z – vector of measured quantities, $z = \begin{bmatrix} \Delta B \\ \Delta L \\ \Delta h \end{bmatrix} m$, $x(k)$ – parameters determined a posteriori, $P(k)$ – covariance matrix of the parameters determined a posteriori.

In the analyzed case, vector z represents the difference between the estimated user coordinates from the GPS/SBAS solution and the flight reference position. In addition, during the calculations, the horizontal components B and L were converted from degrees to meters in order to standardize the units. Equation 6 defines the prediction stage, while Equation 7 defines the correction stage. In aviation applications within GPS/SBAS positioning, Kalman filtering allows for:

- determining the coordinates when reference position of the airplane is unknown,
- or filtering the difference between the estimated coordinates and reference flight position when the reference position of the aircraft is known [15].

In practice, the second method was used, which is simpler, significantly speeds up calculations, and simplifies the observation model. The Kalman filter is implemented when all measurements are observed, including the vector z. Therefore, the algorithm is effective when having all measurements in all measurement epochs of the research experiment.

Algorithms (1–7) have already been used, among others, in works [10, 15, 28], which

presented a multi-receiver GPS/SBAS solution. However, it is worth noting what distinguishes the presented algorithm from works [10, 15, 28]. In [10], the research methodology was based only on algorithms (1–2) for a dual-receiver GPS/EGNOS solution. Position errors were calculated separately for each GNSS receiver and then integrated into a mathematical model. In turn, in [15], algorithms (1–2) and algorithms (6–7) were also used to determine the accuracy of static positioning, separately from the GPS/EGNOS and GPS/SDCM solutions. Additionally, in [28], algorithms (3–4) and (6–7) were used to increase the accuracy of kinematic positioning of a car only for the multi-receiver GPS/EGNOS solution. Now, comparing the methodology of this article with the works [10, 15, 28], it can be noted that:

- this paper combines all algorithms (1–7) that were presented separately in publications [10, 15, 28],
- a mathematical description of the kinematic position based on all possible GPS/SBAS solutions for two GNSS receivers was provided,
- the methodology has been extended to include aerial surveys using a multi-receiver solution not only for GPS/EGNOS, but also for GPS/SDCM.
- the experimental nature of the methodology was emphasized as typically aerial, rather than just static geodetic [15] or automotive navigation [28].

RESEARCH TEST

The research methodology described in Chapter 3 was tested in an aerial experiment conducted at the EPOD (European Poland Olsztyn Dajtki) airport using a Diamond DA 20-C aircraft. Two geodetic multi-system and multi-frequency GNSS receivers, i.e., Trimble Alloy and Septentrio AsterRx2i [30], were installed on board the aircraft. Both GNSS receivers are also capable of recording SBAS data, which was used in this study. Figure 2 shows the aircraft with GNSS receivers installed just before takeoff. The flight took place in northeastern Poland in the Warmian-Masurian and Podlaskie provinces, as shown in Figure 3. The flight lasted approximately 12721 s, which is about 3.5 hours. Each measurement epoch was recorded at 1-second intervals. During the flight, both GNSS receivers collected the GPS and SBAS data at 1-second intervals for kinematic research purposes.

Next, the GPS/SBAS data was applied to solve the aircraft position based on absolute SPP method [32]. The determined coordinates were referenced to BLh geodetic coordinates [33]. The model of the SPP method was executed in RTKLIB v.2.4.3 geodetic software [34]. During the calculations in the RTKLIB software, GPS/EGNOS and GPS/SDCM position solutions were obtained for two GNSS receivers. In addition, a reference position was obtained in parallel from the MAGNET Tools v.5.1.1.0 software [35]. The calculations used precise GPS phase observations from on-board GNSS receivers and from the OPNT reference station of the ASG-EUPOS system [36]. The reference flight trajectory was determined with an accuracy greater than 0.1 m for BLh components. The coordinates from the individual GPS/SBAS solution and the reference flight position were then compared to calculate position errors according to Equations 1–4. At this point, the calculations are performed in a proprietary script written in the Scilab v.6.1.1

Figure 2. The Diamond DA 20-C aircraft with on-board GNSS receivers [photo by: A. Ciećko]

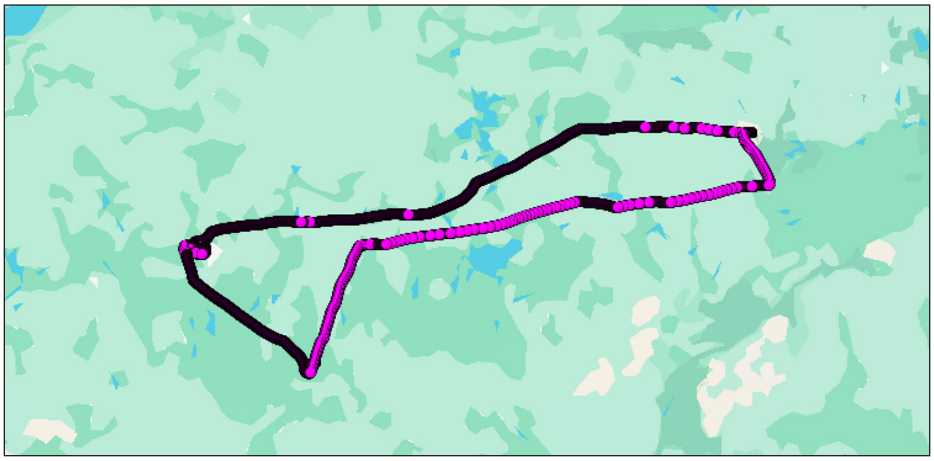

Figure 3. The flight path of airplane [31]

environment [37]. In addition, commands are executed to apply the Kalman filter to increase positioning accuracy. All graphs, starting with Figure 4, were created using graphical functions also in the Scilab language.

RESEARCH RESULTS

The analysis of the test results first shows the satellites number in the GPS/EGNOS and GPS/SDCM models for both GNSS receivers, as shown in Figures 4–5. For the Septentrio receiver, the number of satellites in the GPS/EGNOS solution ranged from 5 to 13. The satellites number in the GPS/SDCM model ranged from 4 to 9. For the Trimble receiver, satellites number in the GPS/EGNOS solution ranged from 7 to 13. The number of GPS satellites tracked with SDCM corrections ranged from 5 to 9. For both GNSS receivers, a larger number of satellites was noticeable for the GPS/EGNOS solution. A similar configuration of GPS satellites with EGNOS and SDCM corrections can be seen in [15].

Figure 6 shows the position errors obtained from Equations 1–4. The accuracy for BLh

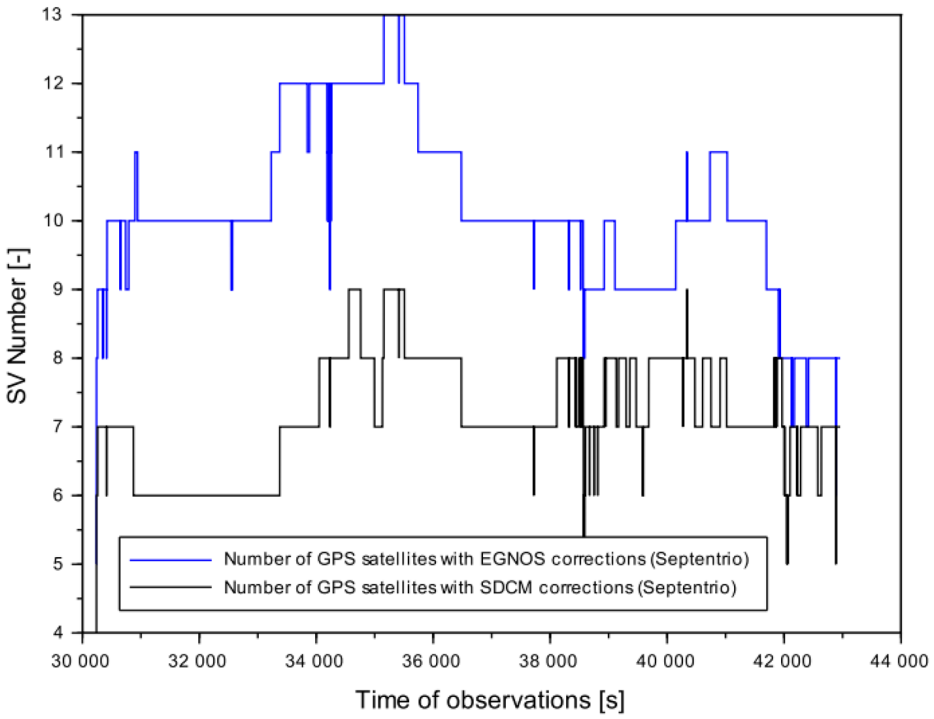

Figure 4. Number of satellites tracked by a Septentrio receiver

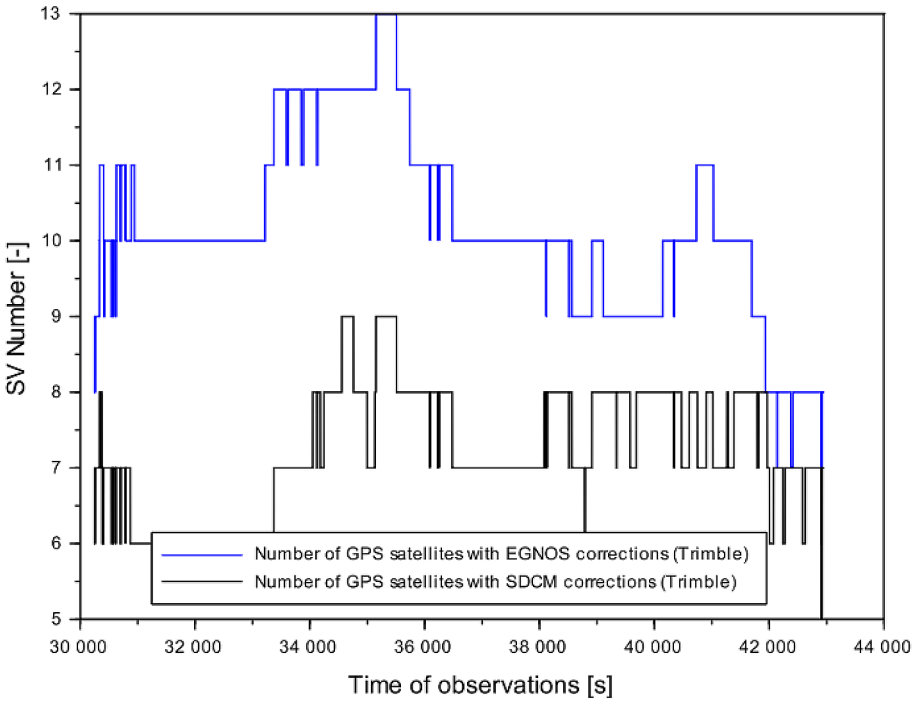

Figure 5. Number of satellites tracked by a Trimble receiver

coordinates equaled to: 1.60 m for component B, 1.69 m for component L, and 2.94 m for component h. The largest position errors are visible in the initial phase of flight. At that time, both receivers tracked the smallest number of GPS satellites, 4 and 5, respectively. Next, Figures 7–8 show the position errors obtained against Kalman filtering. Position errors (ΔB, ΔL, Δh) from Equation 4 are marked in blue, while those after Kalman filtering are marked in red. As a result of applying the Kalman filter, the position errors were: up to 1.45 m for the ΔB parameter, up to 1.44 m for the ΔL parameter, and up to 2.35 m for the Δh parameter. Therefore, the Kalman filter

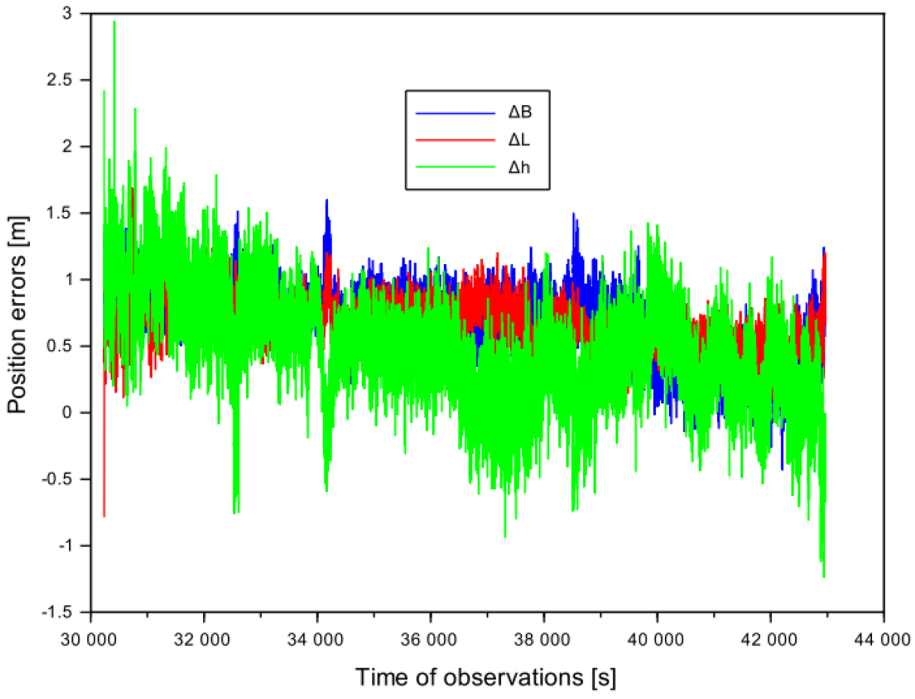

Figure 6. Position errors of airplane coordinates

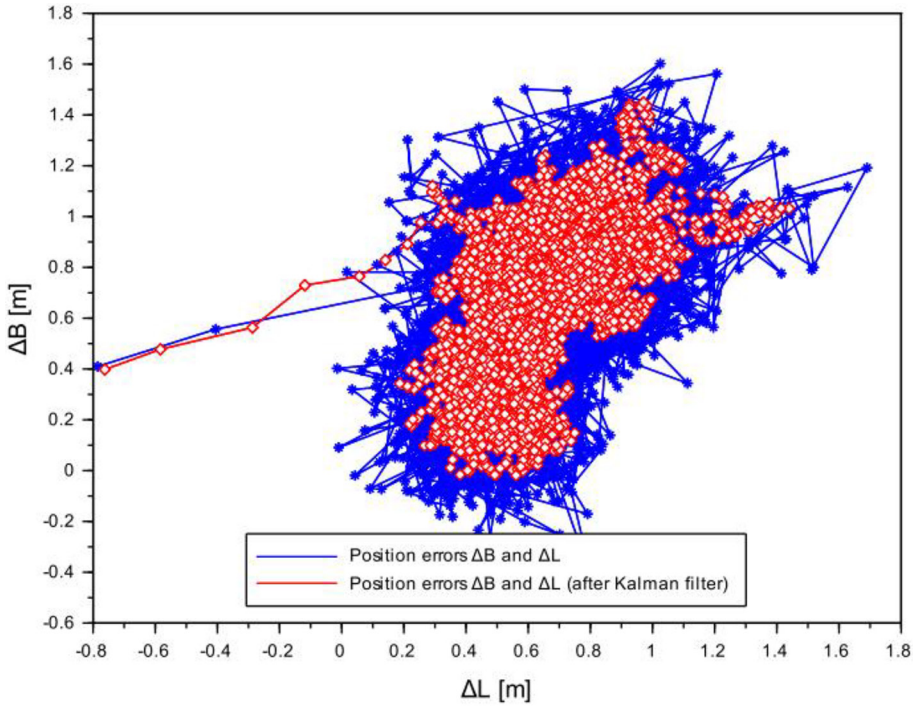

Figure 7. Position errors of horizontal airplane coordinates

algorithm reduced position errors for horizontal components by 9% for coordinate B and 14% for coordinate L. In addition, position errors for component h were reduced by 20%. In total, Kalman filtering reduced position errors by:

- in 6381 measurement epochs for coordinate B, which accounts for over 50% of all measurement epochs recorded during the flight,
- in 6444 measurement epochs for coordinate L, which accounts for over 51% of all measurement epochs recorded during the flight,
- in 6398 measurement epochs for the h coordinate, which accounts for over 50% of all

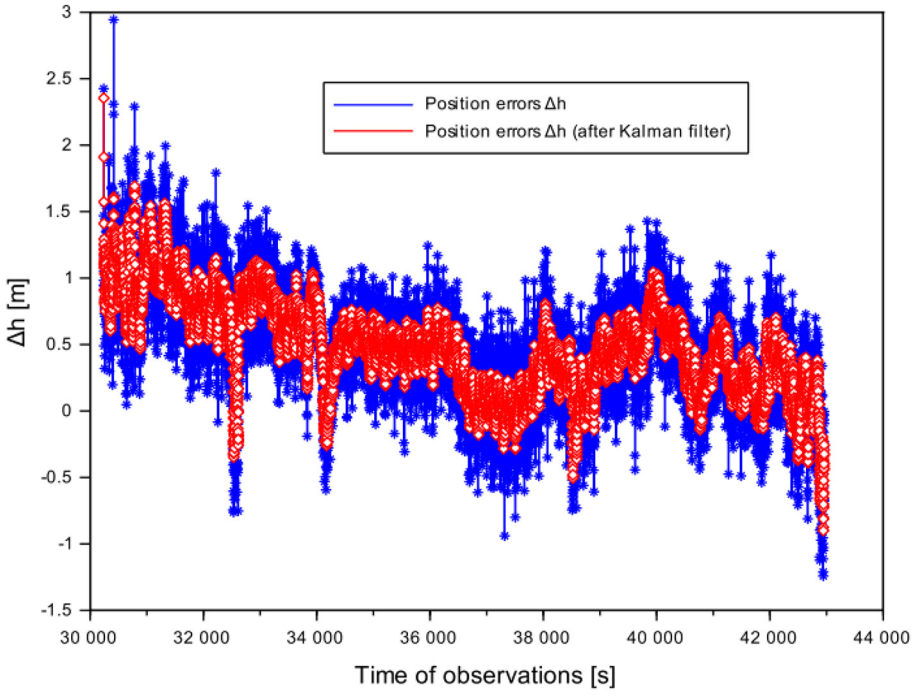

Figure 8. Position errors of vertical airplane coordinates

measurement epochs recorded during the flight.

It is also worth noting that in the flight final stage, the accuracy of position determination increases compared to the first phase of the flight.

DISCUSSION

The chapter discussing the results has been divided into three main thematic threads, namely:

- extended statistical analysis of accuracy term,
- demonstrating the characteristics of SBAS corrections in terms of determining the accuracy parameter,
- comparing the accuracy results and other quality parameters with the ICAO requirements for SBAS applications in aviation,
- development of a research methodology for the weighted average model,
- comparing the accuracy results obtained with the state of the art analysis.

Extended statistical analysis of accuracy parameter

In the previous chapter, Figures 6–8 showed only basic accuracy measures in the form of position errors. In this chapter, other accuracy measures in the form of statistical errors were presented: MAE [38], MAX [13], RMS [39], 1σ (at a confidence level of 68%) and 2σ (at a confidence level of 95%) [40]. Table 1 shows the individual values of statistical error measures before and after filtering. After Kalman filtering, all statistical errors were reduced. All calculated accuracy measures refer to the determined position errors (ΔB, ΔL, Δh). It is worth noting that the RMS error and 1σ standard deviation values were determined to be below 1 m. In aviation navigation applications, these are very satisfactory figures.

Table 1. Statistical measures of errors

Statistical parameter	Before Kalman filter operation	After Kalman filter operation
MAE [m]	ΔB = 0.71 ΔL = 0.67 Δh = 0.49	ΔB = 0.70 ΔL = 0.66 Δh = 0.48
MAX [m]	ΔB = 1.60 ΔL = 1.69 Δh = 2.94	ΔB = 1.45 ΔL = 1.44 Δh = 2.35
RMS [m]	ΔB = 0.75 ΔL = 0.69 Δh = 0.63	ΔB = 0.74 ΔL = 0.68 Δh = 0.60
1σ [m]	ΔB = 0.27 ΔL = 0.18 Δh = 0.41	ΔB = 0.24 ΔL = 0.16 Δh = 0.35
2σ [m]	ΔB = 0.54 ΔL = 0.36 Δh = 0.82	ΔB = 0.48 ΔL = 0.32 Δh = 0.70

Characteristics of SBAS corrections in terms of determining the accuracy parameter

The accuracy of the GPS/EGNOS+GPS/SDCM solution depends mainly on individual SBAS correction values [41]. These include long-term corrections to satellite ephemeris and satellite clock error [42–44], fast corrections to satellite ephemeris and satellite clock error [24, 45], SBAS ionospheric correction [46, 47], and SBAS tropospheric delay based on the RTCA-MOPS model [48, 49]. It is worth noting at this point that the above-mentioned parameters modify the basic observation equation in the SPP code method [50]. Thus, the satellite ephemeris and satellite clock bias are updated with long-term and fast SBAS corrections [27]. In addition, atmospheric delays are calculated as the SBAS ionospheric model and SBAS tropospheric correction [30]. It is therefore worth analyzing the individual types of SBAS corrections. Figures 9–11 show the values of long-term SBAS data to GPS satellite position in orbit [24, 51]. In this case, the arithmetic mean of EGNOS and SDCM corrections for the geocentric XYZ coordinates of a GPS satellite was determined. The analysis was performed for 14 GPS satellites with PRN numbers: PRN1, PRN2, PRN3, PRN6, PRN7, PRN8, PRN9, PRN12, PRN17, PRN21, PRN25, PRN26, PRN31, PRN32. It should be noted that during the flight, SBAS corrections were generated for these GPS satellites from the EGNOS and SDCM support systems. Along the X axis of the GPS satellite position, the correction values changed between -1.875 m to 3.625 m in EGNOS system, and between -0.812 m to 0.500 m in SDCM system. In turn, for the Y component of the GPS satellite position, the correction values changed between -1.625 m to 3.187 m from the EGNOS system, and between -1.312 m to 0.937 m from the SDCM system. For the Z component of the GPS satellite position, the corrections changed from -2.312 m to 3.375 m in EGNOS system and from -1.187 m to 1.250 m in SDCM system. On the basis of Figures 9–11, it can be seen that the spread of SBAS corrections is greater in the EGNOS augmentation system than in the SDCM system. This is confirmed

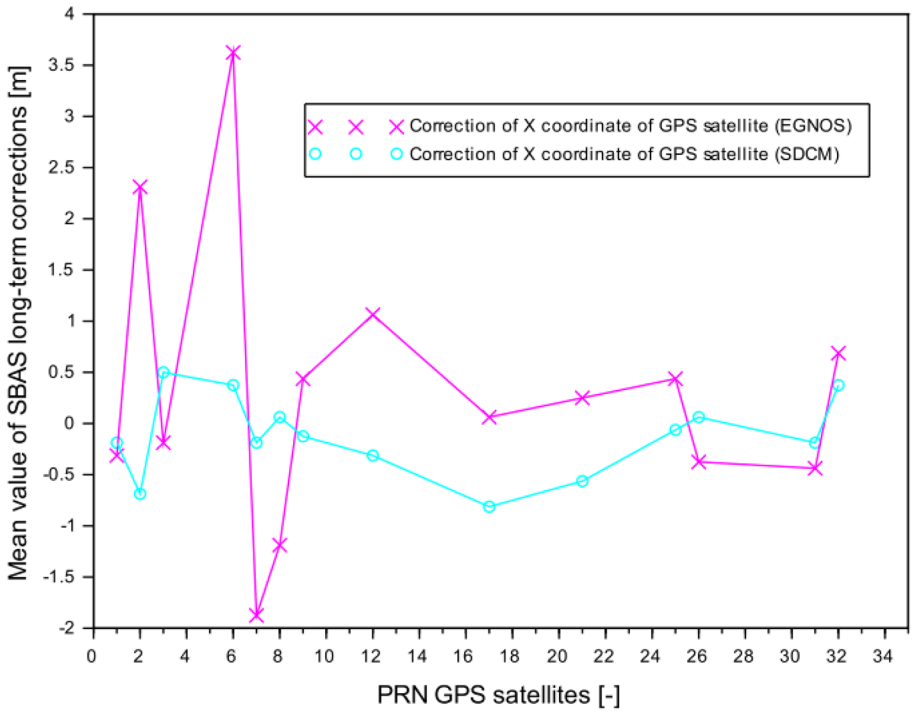

Figure 9. SBAS long-term corrections for X coordinate of GPS satellites

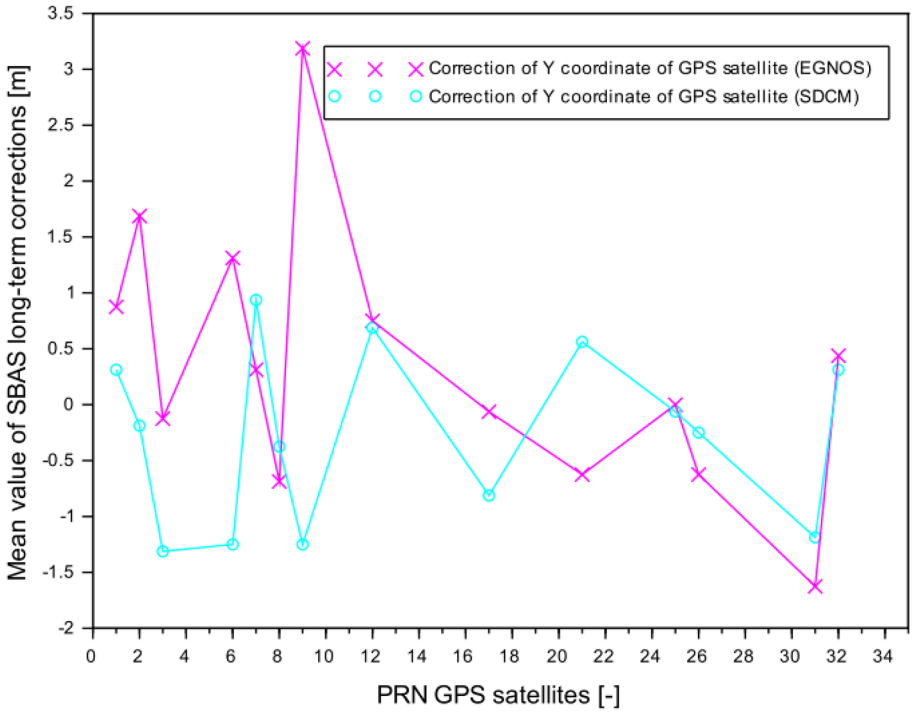

Figure 10. SBAS long-term corrections for Y coordinate of GPS satellites

by calculations and studies carried out as part of [24]. Importantly, the impact of long-term SBAS corrections through ephemeris data correction will be visible for determining the geometric distance in the SPP code method [30, 50]. Next, Figure 12 shows the values of long-term EGNOS and SDCM corrections for GPS satellite clock error correction [24, 52, 53]. The analysis during the experiment was performed for 14 GPS satellites with PRN numbers: PRN1, PRN2, PRN3, PRN6, PRN7, PRN8, PRN9, PRN12, PRN17, PRN21, PRN25, PRN26, PRN31, PRN32. In the case of

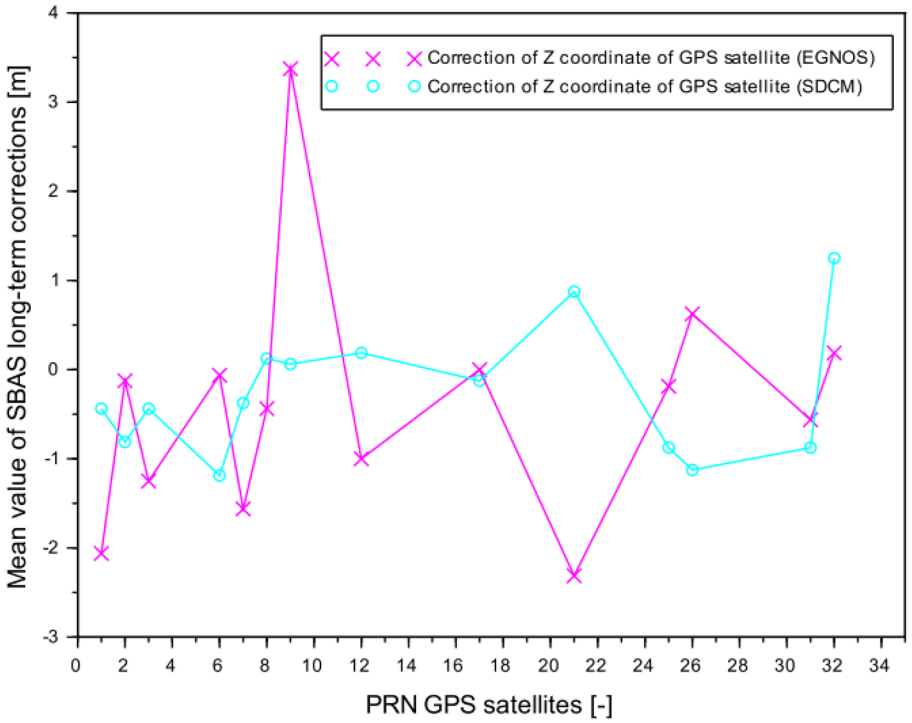

Figure 11. SBAS long-term corrections for Z coordinate of GPS satellites

the EGNOS augmentation system, corrections to the GPS satellite clock error amounted between -0.209 m to 3.071 m. Similarly, for SDCM, these corrections amounted between -1.256 m to 2.234 m. The differences in the corrections values to the GPS satellite clock error are quite significant between the EGNOS and SDCM systems. In a few cases, e.g., satellites G02, G03, G08, G09, the results of EGNOS and SDCM corrections are similar. The impact of long-term SBAS corrections will be visible for determining the GPS satellite clock error in SPP code method [24, 30, 50].

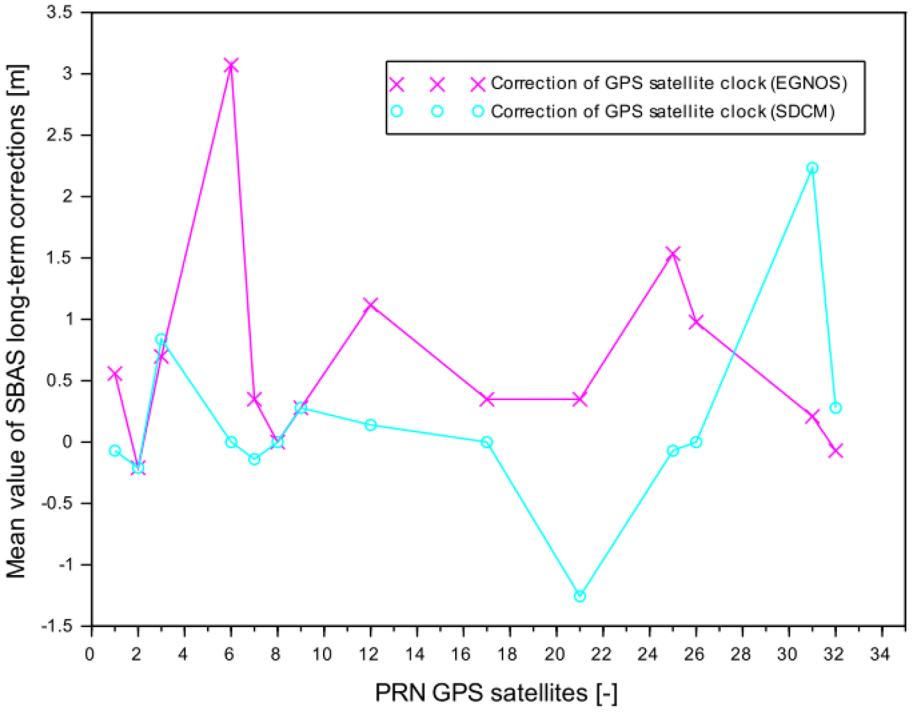

Figure 12. SBAS long-term corrections for clock of GPS satellites

Figure 13 shows the values of EGNOS and SDCM fast corrections [21, 24, 54]. The analysis of SBAS fast corrections was performed for 14 GPS satellites with PRN numbers: PRN1, PRN2, PRN3, PRN6, PRN7, PRN8, PRN9, PRN12, PRN17, PRN21, PRN25, PRN26, PRN31, PRN32. In the case of the EGNOS augmentation system, the fast corrections amounted between -1.750 m to 0.500 m. Similarly, in the SDCM system, these corrections ranged from -4.187 m to 1.375 m. On the basis of Figure 13, it can be seen that the spread of SBAS corrections is greater in the SDCM augmentation system than in the EGNOS system. The impact of fast SBAS corrections will be visible for pseudo-range modifications in the SPP code method [24, 30, 50].

Finally, Figures 14–15 show the ionospheric and tropospheric SBAS corrections. The ionospheric correction in Figure 14 is shown using the VTEC parameter [55]. In this case, the VTEC value is specified in the TECU unit from the regular grid area of the SBAS ionosphere model with a spatial resolution of 5° × 5° [56]. The VTEC values were calculated as a weighted average of four neighboring nodes of the SBAS ionosphere model grid. In the conducted experiment, the VTEC correction value from the EGNOS model ranged from 7.7 TECU to 12.3 TECU, while from the SDCM model it ranged from 8.5 TECU to 13.1 TECU, respectively. During the flight, the VTEC value from both SBAS systems increased continuously. This is because VTEC reaches its maximum value at 2 p.m. local time [57]. Figure 15 shows the results of SBAS tropospheric delay calculated using the RTCA-MOPS model [58]. The tropospheric correction was designated using the ZTD parameter [59] during the flight test. The value of ZTD is determined and given in millimeters [60]. In the analyzed experiment, the ZTD parameter value for the EGNOS system ranged from 2252.1 mm to 2391.4 mm, while for the SDCM system it ranged from 2252.4 mm to 2391.9 mm. The VTEC and ZTD values were determined in the flight test in a similar manner to that described in [24].

Comparison of the accuracy results and other quality parameters with ICAO requirements for SBAS applications in aviation

In this section, the obtained position errors were checked with the ICAO certification requirements [61, 62]. According to the ICAO standards, the accuracy of GPS/SBAS positioning should be:

- less than 16 m for Latitude and Longitude coordinates under landing procedures of SBAS APV-I and SBAS APV-II,

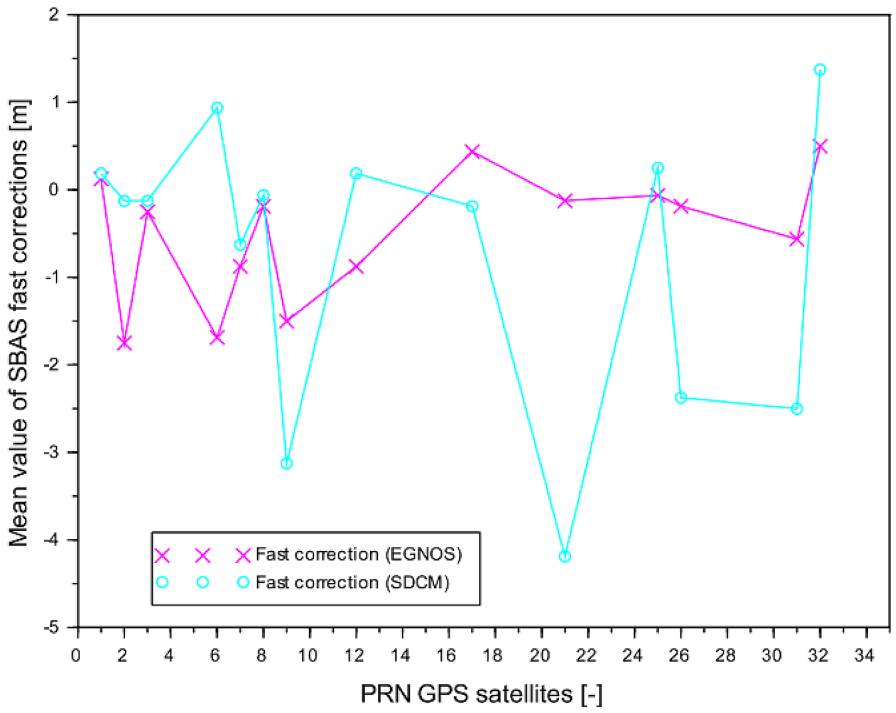

Figure 13. Fast corrections from EGNOS and SDCM augmentation system

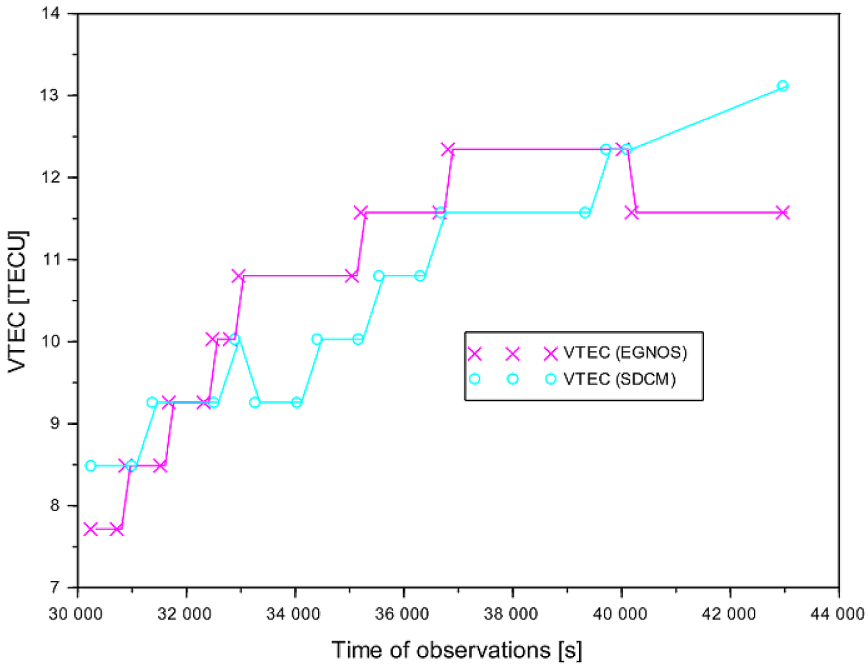

Figure 14. SBAS ionosphere correction from the EGNOS and SDCM augmentation system

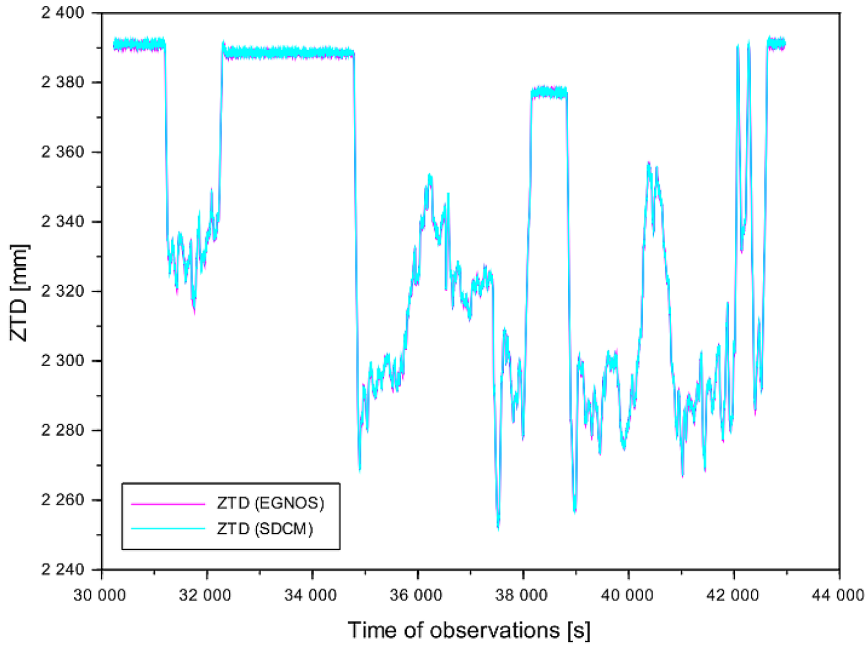

Figure 15. SBAS troposphere correction from the EGNOS and SDCM augmentation system

Table 2. The values of other GPS/SBAS quality parameters

Quality parameter	Before Kalman filter operation	After Kalman filter operation
Availability [%]	$A = 100$	$A = 100$
Continuity [-]	$C = 1$	$C = 1$
Integrity [-]	$I = 1$	$I = 1$
HPL [m]	$HPL < 12.4$	$HPL < 10.6$
VPL [m]	$VPL < 15.7$	$HPL < 12.5$

- less than 20 m and less than 8 m for ellipsoidal height coordinate under landing procedures of SBAS APV-I and SBAS APV-II [63].

In addition, the remaining GPS/SBAS positioning quality parameters should be at least as follows for the SBAS APV-I and SBAS APV-II procedures [27, 64]:

- for integrity $I = 1 - 2 \cdot 10\text{-}7/h$,
- for continuity $C = 1 - 8 \cdot 10^{-6}$/h for 15 s,

- for availability from 0.99 to 1,
- HPL protection levels < 40 m,
- VPL protection levels < 50 m for SBAS APV-I and VPL < 20 m for the SBAS APV-II procedure.

Table 2 presents the results obtained for continuity, availability, and reliability. Continuity and integrity were 1, and availability was 100%. In turn, the HPL protection levels are less than 12.4 m, and the VPL levels are less than 15.7 m. The quality parameters results for dual-receiver GPS/EGNOS+GPS/SDCM positioning solution do not exceed ICAO technical standards. Therefore, the shown research method meets the requirements of ICAO.

Development of a research methodology for the weighted average model

Looking at the developed algorithm (1–4), it can be seen that it is based on the arithmetic mean [30]. This causes a certain problem in assessing the impact of individual GNSS data from each receiver. In the arithmetic mean model, individual GNSS data are treated as equally accurate measurements, which in reality is not entirely true. Each GNSS receiver can:

- store data in a different way, e.g. in parallel or sequentially,
- have built-in internal filters that smooth GNSS observations to reduce measurement noise,
- be a single- or multi-constellation receiver,
- be capable of recording different types of GNSS observations,
- have different refresh rates for GNSS observations and position determination.

On the basis of the arguments above, it is worth trying to apply the weighted average model to determine the accuracy parameter. On this basis, Equation 4 will be transformed into the following form:

$$wB_1 = \frac{1}{mB^2_{GPS/EGNOS,Rx1}}$$

where: wB_1 – measurement weight for Latitude for GPS/EGNOS solution for first receiver, wB_2 – measurement weight for Latitude for GPS/SDCM solution for first receiver, $wB_2 = \frac{1}{mB^2_{GPS/SDCM,Rx1}}$, wB_3 – measurement weight for Latitude for GPS/EGNOS solution for second receiver, $wB_3 = \frac{1}{mB^2_{GPS/EGNOS,Rx2}}$, wB_4 – measurement weight for Latitude for GPS/SDCM solution for second receiver, $wB_4 = \frac{1}{mB^2_{GPS/SDCM,Rx2}}$, wL_1 – measurement weight for Longitude for GPS/EGNOS solution for first receiver, $wL_1 = \frac{1}{mL^2_{GPS/EGNOS,Rx1}}$, wL_2 – measurement weight for Longitude for GPS/SDCM solution for first receiver, $wL_2 = \frac{1}{mL^2_{GPS/SDCM,Rx1}}$, wL_3 – measurement weight for Longitude for GPS/EGNOS solution for second receiver, $wL_3 = \frac{1}{mL^2_{GPS/EGNOS,Rx2}}$, wL_4 – measurement weight for Longitude for GPS/SDCM solution for second receiver, $wL_4 = \frac{1}{mL^2_{GPS/SDCM,Rx2}}$, wh_1 – measurement weight for ellipsoidal height for GPS/EGNOS solution for first receiver, $wh_1 = \frac{1}{mh^2_{GPS/EGNOS,Rx1}}$, wh_2 – measurement weight for ellipsoidal height for GPS/SDCM solution for first receiver, $wh_2 = \frac{1}{mh^2_{GPS/SDCM,Rx1}}$, wh_3 – measurement weight for ellipsoidal height for GPS/EGNOS solution for second receiver, $wh_3 = \frac{1}{mh^2_{GPS/EGNOS,Rx2}}$, wh_4 – measurement weight for ellipsoidal height for GPS/SDCM solution for second receiver, $wh_4 = \frac{1}{mh^2_{GPS/SDCM,Rx2}}$.

Equation 8 includes measurement weights [65], which were determined as the reciprocals of the squares of the mean errors of the estimated

$$\begin{cases} \Delta B = \dfrac{wB_1 \cdot \Delta B^{GPS/EGNOS}_{Rx1} + wB_2 \cdot \Delta B^{GPS/SDCM}_{Rx1} + wB_3 \cdot \Delta B^{GPS/EGNOS}_{Rx2} + wB_4 \cdot \Delta B^{GPS/SDCM}_{Rx2}}{wB_1 + wB_2 + wB_3 + wB_4} \\ \Delta L = \dfrac{wL_1 \cdot \Delta L^{GPS/EGNOS}_{Rx1} + wL_2 \cdot \Delta L^{GPS/SDCM}_{Rx1} + wL_3 \cdot \Delta L^{GPS/EGNOS}_{Rx2} + wL_4 \cdot \Delta L^{GPS/SDCM}_{Rx2}}{wL_1 + wL_2 + wL_3 + wL_4} \\ \Delta h = \dfrac{wh_1 \cdot \Delta h^{GPS/EGNOS}_{Rx1} + wh_2 \cdot \Delta h^{GPS/SDCM}_{Rx1} + wh_3 \cdot \Delta h^{GPS/EGNOS}_{Rx2} + wh_4 \cdot \Delta h^{GPS/SDCM}_{Rx2}}{wh_1 + wh_2 + wh_3 + wh_4} \end{cases} \quad (8)$$

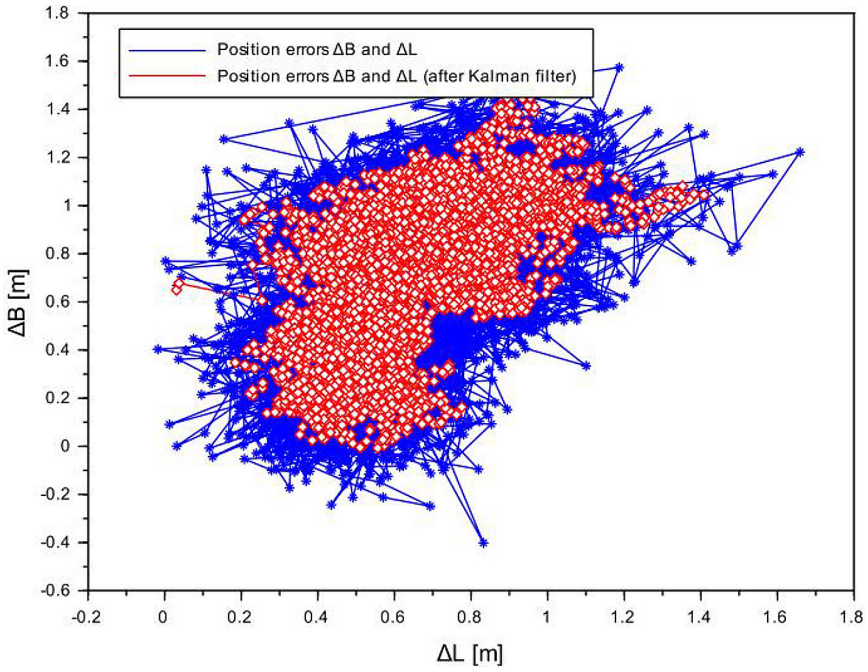

Figure 16. Position errors of horizontal airplane coordinates from weighted mean model

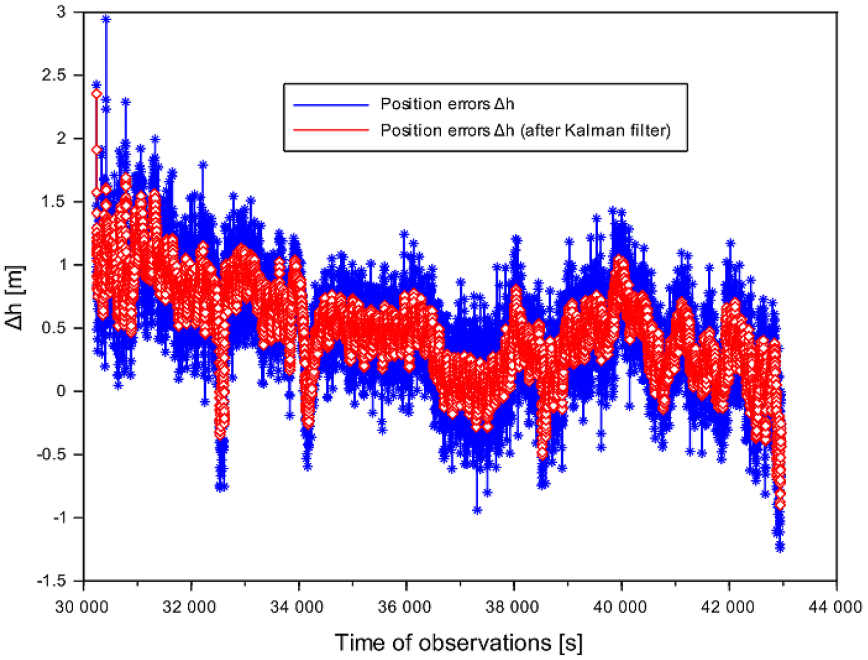

Figure 17. Position errors of vertical airplane coordinates from weighted mean model

coordinates [66]. In this case, Equation 8 provides a solution based on measurements of varying accuracy. The mean errors were determined from a single GPS/EGNOS and GPS/SDCM solution for each GNSS receiver [67].

Figures 16–17 show the results of GPS/EGNOS+GPS/SDCM positioning accuracy from the weighted average model. For the weighted average model, the position errors are:

- from -0.40 m to 1.62 m for the B component,
- from -0.02 m to 1.66 m for the L component,
- from -1.19 m to 2.84 m for the h component.

As a result of Kalman filtering, position errors are less than: 1.47 m for coordinate B, 1.41 m for coordinate L, and 1.97 m for height h. The errors in horizontal coordinates B and L are very close to the results from the arithmetic mean model. However, it is necessary to discuss the accuracy of the vertical component h. In the

case of the arithmetic mean model, a maximum accuracy of the h component equal to Δh = 2.94 m without filtration and Δh = 2.35 m after Kalman filtering were obtained. In turn, the weighted average model yielded Δh = 2.84 m without filtration and Δh = 1.97 m after Kalman filtering. This shows that the weighted average model better fits the ellipsoidal height results relative to the flight reference position. Furthermore, the weighted average model improved the accuracy of the altitude results by 3% without filtering and by 16% after Kalman filtering. Better accuracy results are extremely important for flight safety in the vertical plane. This, in turn, can be directly related to ICAO certification requirements for aviation [27, 30]. Ensuring improved determinability of altitude h may prove to be extremely important in the approach procedure for landing using SBAS support systems. Emphasizing the use of the weighted average model therefore becomes extremely important for calculating the correct flight altitude of an aircraft.

Comparison of the accuracy results obtained with the state of art analysis

The final element of the discussion is to show how the research results relate to the current literature on the subject. From a comparison, it can be seen that:

- at least two SBAS support systems were used in the research, as in publications [7–21],
- the research focused on improving the GPS/SBAS kinematic positioning accuracy algorithm, as in [8–14, 28, 30],
- the research algorithm used a Kalman filter, as in [14, 15, 24, 28],
- owing to the use of the presented research method, higher GPS/SBAS positioning accuracy was achieved than, for example, in works [2, 23, 68, 69],
- owing to the use of the presented research method, higher or comparable GPS/SBAS positioning accuracy was achieved than, for example, in works [8–14, 24, 28, 30],
- this publication is part of further research on the use of the SBAS augmentation systems in aviation in Poland, similar to the works [7–15],
- an advantage of the research conducted was the use of two receivers with an SBAS positioning module, compared to works [2, 13, 14, 24, 47, 63], which used single-receiver GPS/SBAS positioning,
- another advantage of the work is the use of corrections from two SBAS systems, in comparison to publications [2, 4, 5, 22, 23, 26, 28, 61], in which only a single SBAS was used,
- a huge advantage of this work is the demonstration of the characteristics of EGNOS and SDCM corrections during aircraft flight, which can be directly related to publication [24], in which EGNOS and SDCM corrections were calculated, but for a UAV platform.

The article uses a GPS constellation with SBAS corrections. It should be noted that the GPS system, as the primary navigation system according to ICAO, is the fundamental GNSS satellite system for the SBAS systems. Therefore, corrections from the EGNOS and SDCM systems, as well as other SBAS systems, are currently widely adapted for GPS observations. In addition, most GNSS observation processing software uses GPS data and SBAS corrections in the SPP algorithm. Of course, with the development of the GNSS constellation, SBAS corrections will also be adapted to the given global GNSS satellite navigation system in the future. What is more, SBAS corrections will be available not only on the L1 frequency, but also on the L5 frequency. This will primarily allow for the determination and monitoring of ionospheric corrections in real time in the form of the VTEC parameter. This will enable the research to be conducted as part of the DFMC project [70]. Currently, SBAS corrections are used on the L1 frequency in the SPP positioning method. This poses certain limitations in terms of SPP code positioning. Therefore, when the SBAS system is not working, GPS/SBAS positioning in aviation is not possible. Therefore, in addition to monitoring the GPS constellation, SBAS geostationary satellites must also be monitored. For aviation, the limitation of access to SBAS corrections is particularly burdensome in landing approach applications.

CONCLUSIONS

The article presented a methodology for testing and determining the accuracy parameter for the SBAS systems based on a dual-receiver GNSS solution. In particular, it shows a calculation scheme for improving GPS/EGNOS+GPS/SDCM positioning in aviation application. The presented algorithm includes the determination

of position errors of airplane position. Additionally, the determined position errors were filtered to eliminate random and outlier errors from the given time series of data. A linear Kalman filter was used for this purpose. As a final stage of the research, the proposed algorithm was also tested only for dual-receiver GPS/EGNOS positioning and separately for GPS/SDCM positioning. The study used the research material collected during a flight on a Diamond DA 20-C airplane. The calculations used RTKLIB v.2.4.3, Topcon MAGNET Tools v.5.1.1.0, and proprietary numerical scripts written in the Scilab v.6.1.1 environment. The research yielded an accuracy of GPS/SBAS dual-receiver solution better than 2.94 m. After Kalman filtering, position errors were reduced to 14% for horizontal components and 20% for ellipsoidal height. This allowed for a reduction in position errors below 2.35 m. The paper also calculated other statistical errors, such as: MAE, RMS or standard deviation. The article also presented the characteristics of EGNOS and SDCM corrections during the research experiment. The research method in the paper can be used in aviation to increase the accuracy of aircraft positioning using a multi-receiver GNSS solution. Future flight tests will be extended to other SBAS systems. Further recommendations for future research should include:

- integration of the SBAS data also from the UK SBAS and AL-SBAS augmentation systems in precise GPS/SBAS positioning,
- monitoring of SBAS corrections from the EGNOS and SDCM augmentation systems and others,
- comparison of SBAS corrections from the EGNOS, SDCM, UK SBAS, and AL-SBAS augmentation systems,
- implementation of corrections in real-time UAV positioning,
- testing of SBAS corrections with other global GNSS systems.

In terms of the limitations of the presented research method, it should be emphasized that:

- the research method is verifiable for a minimum of two GNSS receivers,
- it is necessary to use corrections from two SBAS systems in the research,
- the developed algorithm must be functional with a Kalman filter,
- the accuracy parameter and other GPS/SBAS positioning quality parameters must be monitored in the research in terms of the ICAO certification requirements.

REFERENCES

1. Specht M., Szmagliński J., Specht C., Koc W., Wilk A., Czaplewski K., Karwowski K., Dąbrowski P., Chrostowski P., Grulkowski S. Analysis of positioning methods using Global Navigation Satellite Systems (GNSS) in Polish State Railways (PKP), Scientific Journals Maritime University of Szczecin, Zeszyty Naukowe Akademia Morska w Szczecinie, 2020, 62(134), 26–35, https://doi.org/10.17402/416
2. Ćwiklak J., Oszczak S., Ciećko A., Popielarczyk D., Grzegorzewski M. Determination of aircraft flight trajectory with radar, GPS OTF and EGNOS positioning, In Proceedings of the European Navigation Conference GNSS 2004, 16–19 May Rotterdam, CD ROM Proceedings.
3. IGS website. MGEX Constellations. Available from: https://igs.org/mgex/constellations/#sbas, (Accessed: 30.12.2025).
4. Lim C.-S., Seok H.-J., Hwang H.-Y., Park B.-W. Prediction on the effect of multi-constellation SBAS by the application of SDCM in Korea and its performance evaluation, Journal of Advanced Navigation Technology, 2016, 20(5), 417–424, https://doi.org/10.12673/jant.2016.20.5.417
5. Siergiejczyk M., Rosiński A., Krzykowska K. Reliability Assessment of Supporting Satellite System EGNOS, In: New Results in Dependability and Computer Systems. Advances in Intelligent Systems and Computing, eds.: W. Zamojski, J. Mazurkiewicz, J. Sugier, T. Walkowiak and J. Kacprzyk, Springer, Heidelberg, 2013, 224, 353–363, https://doi.org/10.1007/978-3-319-00945-2_32
6. Jafernik H., Krasuski K., Michta J. Assessment of suitability of radionavigation devices used in air, Scientific Journal of Silesian University of Technology. Series Transport, 2016, 90, 99–112, https://doi.org/10.20858/sjsutst.2016.90.9
7. Krasuski K., Kirschenstein M. Examination of different models of troposphere delays in SBAS positioning in aerial navigation, Scientific Journal of Silesian University of Technology. Series Transport, 2023, 118, 123–137, https://doi.org/10.20858/sjsutst.2023.118.9
8. Krasuski K., Mrozik M., Wierzbicki D., Ćwiklak J., Kozuba J., Ciećko A. Designation of the quality of EGNOS+SDCM satellite positioning in the approach to landing procedure, *Applied Sciences,* 2022, *12,* 1335, https://doi.org/10.3390/app12031335
9. Mrozik M., Kozuba J., Krasuski K., Ćwiklak J., Bakuła M., Ciećko A., Grunwald G., Wierzbicki D. Analysis of the accuracy of EGNOS+SDCM positioning in aerial navigation, Archives of Transport, 2022, 64(4), 135–144, https://doi.org/10.5604/01.3001.0016.2028
10. Krasuski K., Ćwiklak J., Bakuła M., Mrozik M. Analysis of the determination of the accuracy

parameter for dual receivers based on EGNOS solution in aerial navigation, Acta Mechanica et Automatica, 2022, 16(4), 365–372, https://doi.org/10.2478/ama-2022-0043

11. Krasuski K., Ciećko A., Bakuła M., Grunwald G. Accuracy examination of the SDCM augmentation system in aerial navigation, Energies, 2022, 15, 7776, https://doi.org/10.3390/en15207776
12. Krasuski K., Lalak M., Gołda P., Ciećko A., Grunwald G., Mrozik M., Kozuba J. Analysis of the precision of determination of aircraft coordinates using EGNOS+SDCM solution, Archives of Transport, 2023, 67(3), 105–117, https://doi.org/10.5604/01.3001.0053.7264
13. Krasuski K., Wierzbicki D., Bakuła M. Improvement of UAV positioning performance based on EGNOS+SDCM solution, *Remote Sensing*, 2021, 13, 2597, https://doi.org/10.3390/rs13132597
14. Krasuski K., Bakuła M., Ciećko A., Grunwald G., Gołda P., Mrozik M., Kozuba J. Algorithms to improve unmanned aerial vehicle positioning accuracy using European Geostationary Navigation Overlay Service and System for Differential Corrections and Monitoring ionospheric corrections, Advances in Science and Technology Research Journal, 2025, 19(1), 284–300, https://doi.org/10.12913/22998624/195195
15. Bakuła M., Krasuski K., Dawidowicz K. Dual Receiver EGNOS+SDCM Positioning with C1C and C1W Pseudo-Range Measurements, *Remote Sensing*, 2022, 14, 3152, https://doi.org/10.3390/rs14133152
16. Januszewski J. Satellite navigation systems in the transport, today and in the future, Archives of Transport, 2010, 22(2), 175–187, https://doi.org/10.2478/v10174-010-0011-4
17. Januszewski J. A Look at the development of GNSS capabilities over the next 10 years, TransNav: International Journal on Marine Navigation and Safety of Sea Transportation, 2011, 5(1), 73–78.
18. Walter T., Blanch J., Enge P. Coverage Improvement for Dual Frequency SBAS, In *Proceedings of the 2010 International Technical Meeting of The Institute of Navigation*, San Diego, CA, January 2010, 344–353.
19. Kim Y.-G., Park K.-D. Evaluation of SBAS Positioning Performance According to the Service Region: WAAS, MSAS, EGNOS, SDCM and GAGAN, In Proceedings of the ISGNSS 2019 in Conjunction with IPNT Conference, Jeju, Korea, 29 October–1 November 2019, 347–350.
20. Pandele A., Croitoru A., Ion M., Buehler S. ROSISMON: Results and Multi-SBAS Fusion at user Level for Non-SoL Applications, In Proceedings of the 31st International Technical Meeting of the Satellite Division of The Institute of Navigation (ION GNSS+ 2018), Miami, FL, USA, 24–28 September 2018, 1124–1143.
21. Nie Z., Zhou P., Liu F., Wang Z. Gao Y. Evaluation of orbit, clock and ionospheric corrections from five currently available SBAS L1 services: Methodology and analysis, *Remote Sensing*, 2019, 11, 411, https://doi.org/10.3390/rs11040411
22. Fellner A., Jafernik H. Airborne measurement system during validation of EGNOS/GNSS essential parameters in landing, Reports on Geodesy and Geoinformatics, 2014, 96, 27–37, https://doi.org/10.2478/rgg-2014-0004
23. Grzegorzewski M. Navigating an aircraft by means of a position potential in three dimensional space, Annual of Navigation, 2005, 9, 1–111.
24. Krasuski K. Algorithms for improving GPS/SBAS positioning accuracy using EGNOS and SDCM augmentation systems, Polish Air Force University Publishing House, 2025, 1–147, https://doi.org/10.55676/68629-06-4. (in Polish)
25. Specht M. Determination of navigation system positioning accuracy using the reliability method based on real measurements, *Remote Sensing*, 2021, 13, 4424, https://doi.org/10.3390/rs13214424
26. Fellner R. Analysis of the EGNOS/GNSS parameters in selected aspects of Polish transport, Transport Problems, 2014, 4(9), 27–37.
27. International Civil Aviation Organization. ICAO Standards and Recommended Practices (SARPS), Annex 10, Volume I (Radio Navigation Aids), 2006. Available from: http://www.ulc.gov.pl/pl/prawo/prawomi%C4%99dzynarodowe/206-konwencje, (Accessed: 13.12.2025).
28. Ciećko A., Bakuła M., Grunwald G., Ćwiklak J. Examination of Multi-Receiver GPS/EGNOS Positioning with Kalman Filtering and Validation Based on CORS Stations, Sensors, 2020, 20, 2732, https://doi.org/10.3390/s20092732
29. Kaniewski P. Adaptive Kalman filter of GNSS receiver, Logistyka, 2011, 6, 1569–1578. (in Polish).
30. Mrozik M. Application of the SBAS positioning method in the aircraft approach procedure, Ph.D. thesis, Silesian University of Technology, Gliwice, Poland, 2023. (in Polish).
31. Google Earth website. Available from: https://earth.google.com/web/@54.29577909,20.85837908,0a,598238.34321047d,30.00074101y,0h,0t,0r/data=CgRCAggCOgMKATBCAggASggI2o6T4gcQAA?authuser=0, (Accessed: 24.12.2025).
32. Thari P., Satirapod C. Performance assessment of second-generation SBAS prototype in Thailand. Geomatics and Environmental Engineering, 2025, 19(6), 75–95, https://doi.org/10.7494/geom.2025.19.6.75
33. Takasu T. RTKLIB ver. 2.4.2 Manual, RTKLIB: An Open Source Program. Package for GNSS

Positioning, 2013. Available from: http://www.rtklib.com/prog/manual_2.4.2.pdf, (Accessed: 24.12.2025).

34. RTKLIB webiste. Avialable from: http://rtklib.com/, (Accessed: 01.12.2025).
35. MAGNET Tools Website. Available from: https://www.topconpositioning.com/office-software-and-services/survey-software/magnet-tools, (Accessed: 30.12.2025).
36. ASG-EUPOS Website. OPNT Olsztyn. Available from: https://www.asgeupos.pl/opnt/, (Accessed: 30.12.2025).
37. Scilab website. Previous versions. Available from: https://www.scilab.org/download/previous-versions, (Accessed: 30.12.2025).
38. Barbero T., Matera E.R., Ekambi B., Chamard J., Ekambi M. Toward an interpretable multipath error model from GNSS observables through the application of deep learning, Eng. Proc., 2026, 126, 14, https://doi.org/10.3390/engproc2026126014
39. Przestrzelski P., Bakuła M., Galas R. The integrated use of GPS/GLONASS observations in network code differential positioning, GPS Solutions, 2017, 21, 627–638, https://doi.org/10.1007/s10291-016-0552-y
40. Specht C. Maritime DGPS system positioning accuracy as a function of the HDOP in the context of hydrographic survey performance. Remote Sensing, 2023, 15, 10, https://doi.org/10.3390/rs15010010
41. Kaźmierczak R., Grunwald G. Distribution of EGNOS corrections in time, Logistyka, 2012, 3, 995–1000. (in Polish)
42. Kim J., Kim M. ARMA prediction of SBAS ephemeris and clock corrections for low earth orbiting satellites, International Journal of Aerospace Engineering, 2015, Article ID 165178, 8 pages, https://doi.org/10.1155/2015/165178
43. Li L., Jia C., Zhao L., Cheng J., Liu J., Ding J. Real-time single frequency precise point positioning using SBAS corrections, Sensors, 2016, 16(8), 1261, https://doi.org/10.3390/s16081261
44. Han D.-H., Kim D.-U., Kim J.-B., Kee C.-D., Choi K.-S., Han, J.-A. Methodology for evaluating SBAS satellite correction. Journal of Positioning, Navigation, and Timing, 2018, 7(4), 277–284, https://doi.org/10.11003/JPNT.2018.7.4.277
45. Park K.W., Park J.I., Park C. Efficient methods of utilizing multi-SBAS corrections in multi-GNSS positioning, Sensors, 2020, 20(1):256, https://doi.org/10.3390/s20010256
46. Kim M., Kim J. SBAS-aided GPS positioning with an extended ionosphere map at the boundaries of WAAS service area. Remote Sens., 2021, 13, 151, https://doi.org/10.3390/rs13010151
47. Sakai T., Kitamura M., Aso T., Hoshinoo K. SBAS Ionospheric Correction with Minimalization of the Ionospheric Threat, In Proceedings of the 2017 International Technical Meeting of The Institute of Navigation, Monterey, California, January 2017, 1049–1056, https://doi.org/10.33012/2017.14943
48. Kim D.-U., Han D.-H., Kee C.-D., Lee C.-S., Lee C.-H. Accuracy verification of the SBAS tropospheric delay correction model for the Korean Region. Journal of Advanced Navigation Technology, 2016, 20(1), 23–28, https://doi.org/10.12673/JANT.2016.20.1.23
49. Narayanan S., Osechas O., Hoque M. M., Authie T., Lopez C. Real-time Capable Tropospheric Modeling for SBAS-PPP, In Proceedings of the 2023 International Technical Meeting of The Institute of Navigation, Long Beach, California, January 2023, 922-936, https://doi.org/10.33012/2023.18616
50. Krasuski K., Wierzbicki D. Application the SBAS/EGNOS Corrections in UAV Positioning, *Energies*, 2021, *14,* 739, https://doi.org/10.3390/en14030739
51. Innac A., Angrisano A., Del Pizzo S., Cappello G., Gaglione S. The EGNOS Augmentation in Maritime Navigation, Sensors, 2022, 22, 775, https://doi.org/10.3390/s22030775
52. Heßelbarth A., Wanninger L. SBAS orbit and satellite clock corrections for precise point positioning, GPS Solutions, 2013, 17, 465–473, https://doi.org/10.1007/s10291-012-0292-6
53. Jeong M.-S., Kim J.-R. Accuracy analysis of SBAS satellite orbit and clock corrections using IGS precise ephemeris, Journal of Advanced Navigation Technology, 2009, 13(2), 178–186.
54. Lim C., Park B., Kee C. Efficiency Improvement of the Current SBAS System by Removal of RRC and Fast Correction, In Proceedings of the 2017 International Technical Meeting of The Institute of Navigation, Monterey, California, January 2017, 619-626, https://doi.org/10.33012/2017.14879
55. Rovira-Garcia A., Juan J. M., Sanz J., González-Casado G., Ibáñez D. Accuracy of ionospheric models used in GNSS and SBAS: methodology and analysis, Journal of Geodesy, 2016, 90, 229–240, https://doi.org/10.1007/s00190-015-0868-3
56. Yin P., Shi S., Ren D. SBAS ionospheric grid delay estimation based on ionospheric tomography: a case study on September 7–9, 2017, GPS Solutions, 2022, 26, 86, https://doi.org/10.1007/s10291-022-01259-7
57. Boisits J., Glaner M., Weber R. Regiomontan: A regional high precision ionosphere delay model and its application in precise point positioning, Sensors, 2020, 20, 2845, https://doi.org/10.3390/s20102845
58. Bosy J., Precise processing of satellite GPS observations in local networks located in mountain areas, Wydawnictwo Akademii Rolniczej we Wrocławiu, Zeszyty Naukowe Akademii Rolniczej we Wrocławiu, Nr 522, Seria Rozprawy CCXXXIV, Wrocław, 2005, 1–155. (in Polish)

59. Wielgosz P., Krukowska M., Paziewski J., Krypiak-Gregorczyk A., Stępniak K., Kapłon J., Sierny J., Hadaś T., Bosy J. Performance of ZTD models derived in near real-time from GBAS and meteorological data in GPS fast-static positioning. Measurement Science and Technology, 2013, 24(12), 125802, https://doi.org/10.1088/0957-0233/24/12/125802
60. Klos A., Hunegnaw A., Teferle F. N., Abraha K. E., Ahmed F., Bogusz J. Noise characteristics in Zenith Total Delay from homogeneously reprocessed GPS time series, Atmos. Meas. Tech. Discuss., 2016, 1–28, https://doi.org/10.5194/amt-2016-385
61. Tabti L., Kahlouche S., Benadda B, Beldjilali B. Improvement of single-frequency GPS positioning performance based on EGNOS corrections in Algeria. Journal of Navigation, 2020, 73(4), 846-860, 20202, https://doi.org/10.1017/S037346331900095X
62. Tabti L. Evaluation and comparison of the accuracy and integrity of GPS single-point positioning using EGNOS corrections. J. Indian Soc. Remote Sens., 2025, 53, 2577–2590, https://doi.org/10.1007/s12524-025-02168-1
63. Fellner A., Fellner R., Piechoczek E. Pre-flight validation RNAV GNSS approach procedures for EPKT in "EGNOS APV Mielec project". Scientific Journal of Silesian University of Technology. Series Transport, 2016, 90, 37-46, https://doi.org/10.20858/sjsutst.2016.90.4
64. Zalewski P., Bąk A., Bergmann M. Evolution of maritime GNSS and RNSS performance standards. Remote Sensing, 2022, 14, 5291, https://doi.org/10.3390/rs14215291
65. Gargula T. Adjustment of an integrated geodetic network composed of GNSS vectors and classical terrestrial linear pseudo-observations. Appl. Sci., 2021, 11, 4352, https://doi.org/10.3390/app11104352
66. Gargula T. GPS vector network adjustment on the projection plane of local coordinate system. Infrastruktura i Ekologia Terenów Wiejskich, 2010, 6, 133–144. (in Polish).
67. Krasuski K. Application of the GPS/EGNOS solution for the precise positioning of an aircraft vehicle. Scientific Journal of Silesian University of Technology. Series Transport, 2017, 96, 81–93, https://doi.org/10.20858/sjsutst.2017.96.8
68. Grzegorzewski M., Ciećko A., Oszczak S., Popielarczyk D. Autonomous and EGNOS Positioning Accuracy Determination of Cessna Aircraft on the Edge of EGNOS Coverage, In Proceedings of the 2008 National Technical Meeting of The Institute of Navigation, San Diego, CA, USA, 28–30 January 2008, 407–410.
69. Ciećko A., Grzegorzewski M., Ćwiklak J., Oszczak S., Jafernik H. Air navigation in eastern Poland based on EGNOS, In: Proceedings of the Aviation Technology, Integration, and Operations Conference (ATIO 2013), Los Angeles, CA, USA, 12–14 August 2013; Red Hook: Curran, NY, USA, Volume 1, 603–613, https://doi.org/10.2514/6.2013-4254
70. Mabilleau M., De Sousa R., Dennis J., Farnworth R., Estival P., Salabert F., Salos D. DFMC SBAS approach concept, In: Proceedings of the 34th International Technical Meeting of the Satellite Division of The Institute of Navigation (ION GNSS+ 2021), St. Louis, Missouri, September 2021, 1122-1132, https://doi.org/10.33012/2021.18048